www.czasopisma.pan.pl PAN POLSKA AKADEMIA NAUK www.journals.pan.pl

Arch. Min. Sci. **69** (2024), 4, 745-754

Electronic version (in color) of this paper is available: http://mining.archives.pl

DOI: https://doi.org/10.24425/ams.2024.152582

ZHIYUAN SHEN[1*], CHUNTING WANG[1], ZHENLONG YANG[1]

STUDY ON GUIDED SLOT-ORIENTED HYDRAULIC FRACTURING AND ENHANCED PERMEABILITY APPLICATION TECHNOLOGY IN PINGDINGSHAN COAL MINE

To address the issue of low permeability in the coal seam of Pingdingshan coal mine, this study proposes a directional hydraulic fracturing technique enhanced by a preset guide groove, aimed at improving coal seam extraction efficiency. The COMSOL Multiphysics simulation software is utilized to develop a coupling model that integrates coal rock stress, damage, and permeability during hydraulic fracturing. The study examines the changes in the elastic damage modulus and effective extraction radius under the influence of the guide groove, with field tests conducted on the 24130 working face. Results from both numerical simulations and field tests reveal that the horizontal principal stress exceeds the vertical principal stress under the influence of the guide channel, leading to horizontal tensile fractures in the rock stratum. Post-fracturing, the average gas concentration in the extraction borehole reached 42.4%, with an average pure gas extraction rate of 0.0098 m^3/min, and an effective extraction radius of 3.6 m, aligning well with the simulation results.

Keywords: Directional hydraulic fracturing; gas extraction; extraction radius; COMSOL multiphysics numerical simulation

1. Introduction

As coal seam mining depths increase, gas extraction becomes increasingly challenging, exacerbating coal and gas outburst issues, which significantly impede the safety and efficiency of coal mining operations [1-3]. For coal seams that are deeply buried, possess low permeability, and have difficult gas extraction conditions, enhancing extraction efficiency through strengthening measures becomes essential [4,5]. Current anti-reflection methods in coal seam extraction include

[1] SHENYANG JIANZHU UNIVERSITY, CHINA

* Corresponding author: szy0207@foxmail.com

mining protective layer pressure relief [6,7], drilling-based pressure relief [8,9], high-energy liquid disturbance [10,11], and explosive gas disturbance [12,13] techniques. Among these, hydraulic fracturing technology is widely recognized and applied for pressure relief and permeability enhancement in coal seams.

Typically, hydraulic fracturing technology is applied to hard coal seams, where water injection into boreholes induces cracking within the coal body, thereby increasing its permeability. Zhou et al. [14] conducted field tests on hydraulic fracturing and developed a coupling model for coal seam damage, stress, and seepage for numerical simulation. Their findings indicated that post-fracturing, coal seam permeability increased by 67 times, significantly boosting gas extraction. Ma et al. [15] introduced the "W-S-W" enhanced hydraulic fracturing technology and compared it with conventional hydraulic fracturing, revealing that the gas volume fraction post-"W-S-W" fracturing was 1.2 times higher than that of conventional methods, demonstrating a more pronounced gas extraction effect. Profit et al. [16] constructed a mechanical model for hydraulic fracture propagation and analyzed the impact of various parameters using the fluid-structure coupling discrete element method. Marsden et al. [17] examined the feasibility and effectiveness of nanotechnology in hydraulic fracturing for high-gas mines in Australia. Jia et al. [18] applied the RFPA2D-flow numerical simulation method in Mabao Coal Mine to study the impact of multi-point perforation on hydraulic fracturing, concluding that the effective extraction radius was 3 m. While much research has focused on hydraulic fracturing effects and parameter selection, the application of directional hydraulic fracturing technology remains less explored.

In response, using the 24130 working face of No. 10 in Pingdingshan coal mine as a case study, establishes a coupling model of coal rock stress-damage-permeability during hydraulic fracturing and drainage. COMSOL software is employed to simulate coal body damage and gas extraction during hydraulic fracturing, investigating the impact of guide channels on the fracturing process and the efficacy of directional hydraulic fracturing. The findings are significant for enhancing coal seam permeability, reducing engineering costs, and guiding the application of directional hydraulic fracturing in other mining regions.

2. Numerical simulation theory

2.1. Governing equation of solid stress field

Hydraulic fracturing and gas extraction processes are influenced by changes in coal stress and gas adsorption stress, governed by the Navier equation for gas migration stress fields as follows [19]:

$$Gu_{(i,jj)} + \frac{Gu_{(i,jj)}}{1-2v} - \alpha_m p_{(m,i)} - \alpha_f p_{(f,i)} - K\varepsilon_{(s,i)} + Fi = 0 \tag{1}$$

Where, G is shear modulus, Pa; v is Poisson's ratio; K is the volume modulus of coal and rock, Pa; α_m and α_f are Biot coefficients corresponding to pore and fracture, respectively. Pm is pore fluid pressure, Pa; u is the flow rate of fluid, m/s; ε is the strain of coal rock mass, Pa; F_i is volume force, Pa; P_f is fracture fluid pressure, Pa.

2.2. Damage control physical equation

The coal seam is a heterogeneous elastic material, where pore and fracture damage strain follows a Weibull distribution, with the probability density function given by:

$$f(u) = \frac{m}{u_0}(u/u_0)^{m-1}\exp\left[-(u/u_0)^m\right] \tag{2}$$

Where, u is the unit mechanical parameter; u_0 is the mean value of unit mechanical parameters; m is the homogeneity parameter.

Under high-pressure water injection, coal seam cracks enlarge, reducing the coal body's original elastic modulus. When the stress state indicates compressive and tensile failure, the damage follows the Mohr-Coulomb criterion:

$$F_1 = \delta_1 - f_{t0} \tag{3}$$

$$F_2 = -\sigma_3 + \sigma_1\frac{1+\sin\beta}{1-\sin\beta} \geq f_{c0} \tag{4}$$

Where, σ_1 and σ_3 are the maximum and minimum principal stress, Pa; β is the angle of internal friction; f_{c0} is uniaxial compressive strength, Pa; f_{t0} is compressive strength, Pa; F_1 and F_2 are the damage thresholds.

The damage variable of high-pressure water injection into coal seam is:

$$D = \begin{cases} 0, & F_1 < 0, F_2 < 0 \\ 1-\left|\dfrac{\varepsilon_{t0}}{\sigma_1}\right|^2, & F_1 = 0, F_2 > 0 \\ 1-\left|\dfrac{\varepsilon_{c0}}{\sigma_1}\right|^2, & F_1 = 0, F_2 > 0 \end{cases} \tag{5}$$

Where, ε_{t0} is the maximum tensile principal strain; ε_{c0} is the maximum compressive principal strain.

2.3. Governing equation of seepage field in coal seam

During the processes of forced fracturing and gas extraction, a gas-water two-phase flow phenomenon is observed. Based on Darcy's law, the governing equations describing the gas seepage field and the transport dynamics of gas and water within fractures can be expressed as follows [20]:

$$\frac{\partial}{\partial t}\left(S_g\phi\frac{M_g}{RT}P_g + \frac{V_L P_g}{P_L+P_g}\rho_c\rho_{gs}\right) + \nabla\cdot\left[-\frac{Mg(P_g+b)}{RT}\frac{KK_{rg}}{u_g}\nabla P_{fg}\right] = 0 \tag{6}$$

$$\frac{\partial}{\partial t}(S_w \phi \rho_w) + \nabla \cdot (-\rho_w \frac{K_{rw} K}{u_w} \nabla P_w) = 0 \tag{7}$$

Where, S_g is gas phase saturation; S_w is water phase saturation; K is absolute permeability, m^2; K_{rw} is the relative permeability of water phase. u_g is the dynamic viscosity of gas phase, Pa·s; u_w is the dynamic viscosity of the water phase, Pa·s; b is slip factor, Pa; P_w indicates the water injection pressure (MPa). φ is the fracture porosity; ρ_w is water density, kg/m^3; ρ_c is coal body density, kg/m^3; V_L is Langmuir adsorption volume constant; P_L is Langmuir pressure constant.

3. Numerical simulation of directional hydraulic fracturing

3.1. Geological background

The coal seam at the 24130 working face of the Pingdingshan No. 10 coal mine has an average thickness of 5.44 meters. Its permeability coefficient varies from 0.0165 to 0.0447 $m^2/(MPa^2 \cdot d)$, while the attenuation coefficient ranges between 0.3720 and 0.41 d^{-1}. The initial gas dispersion velocity (ΔP) is between 18.5 and 27.1 mmHg. The seam also has a firmness coefficient (f) between 0.251 and 0.345 and a porosity of 0.032, indicating that it is a challenging coal seam to extract.

3.2. Construction of the numerical model

Based on the specific conditions at the 24130 working face, the COMSOL Multiphysics software was used to construct a numerical model. The model dimensions are 42 meters by 11 meters, with the coal seam having a thickness of 5 meters, and the upper and lower roof layers each having a thickness of 3 meters. The model incorporates three pressure holes, two extraction holes, and two directional control holes. The upper section is influenced by the negative rock pressure from the coal seam, the right side by horizontal pressure, the left side serves as the sliding boundary, and the bottom is the fixed boundary. The outer boundary of the coal seam is permeable. The basic coal seam parameters are provided in TABLE 1.

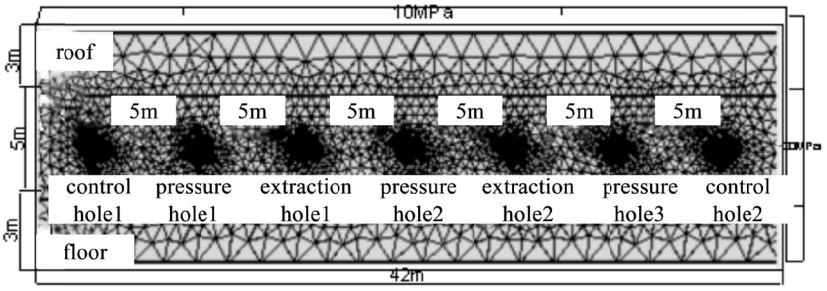

Fig. 1. Physical model of hydraulic fracturing extraction

TABLE 1

Coal seam foundation parameter

Parameter	Value
Initial fracture porosity	0.035
Dynamic viscosity of gas	1.84×10^{-5} Pa·s
Dynamic viscosity of water	0.00103 Pa·s
Langmuir pressure constant	1.85×10^{6} Pa
Langmuir adsorption volume constant	0.0251 m^3/kg
Initial permeability	2.881×10^{-17} m^2
Elastic modulus of skeleton	8.469×10^{9} Pa
Elastic modulus of coal	8.5×10^{9} Pa
Poisson's ratio of coal	0.28
Skeleton density	1270 kg/m^3
Buried depth	450 m
Initial gas pressure	0.41 Mpa
Capillary force	50000 N
Permeability jump coefficient	56
Water injection pressure	20 MPa
Negative gas extraction pressure	18 kPa
Slip factor	0.76×10^{6} Pa
Biot effective coefficient	0.92
Uniformity of coal mass	6 m
Apparent density	1.37 t/m^3

3.3. Description of numerical simulation results

The simulation was carried out with a design water injection pressure of 20 MPa and a negative extraction pressure of 18 kPa. Fig. 2 illustrates the variations in the coal's elastic modulus at different stages of the fracturing process.

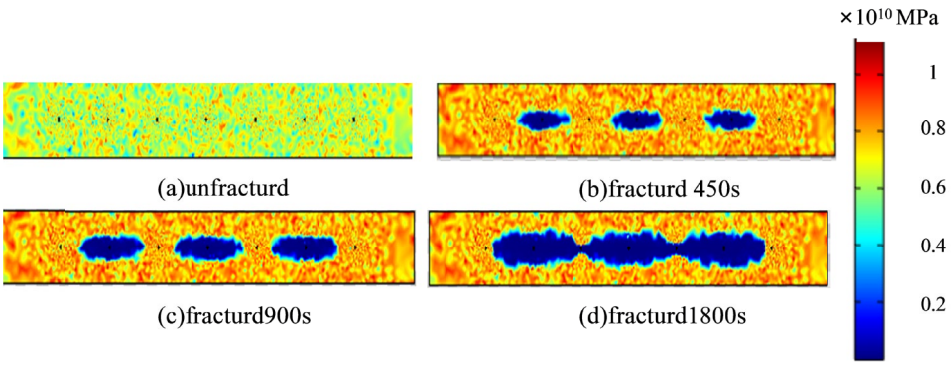

Fig. 2. Elastic modulus of hydraulic fracturing coal

Fig. 2 demonstrates that, upon injecting high-pressure water into the coal rock, the presence of the guiding groove causes the horizontal principal stress to exceed the vertical principal stress. Consequently, tensile fractures in the rock strata initially occur in the horizontal direction. As the injection of high-pressure water continues, the damage zone within the coal seam progressively enlarges in an elliptical pattern. Following this failure, the permeability of the coal rock mass increases.

Fig. 3 illustrates the gas pressure distribution around the extraction hole at various pumping intervals. It shows that the gas pressure near the extraction hole is markedly lower compared to other areas of the coal seam, and the effective extraction area expands as the extraction period progresses. Fig. 4 displays how gas pressure varies with extraction distance over time. The coal seam gas pressure drops by 30% from 0.41 MPa to 0.29 MPa as the extraction radius standard.

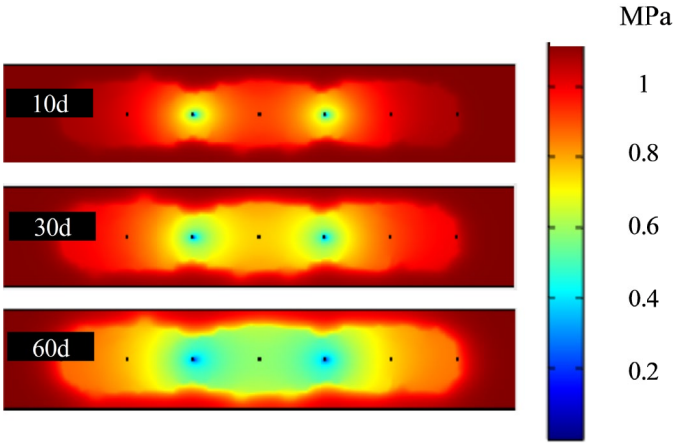

Fig. 3. Gas extraction pressure distribution

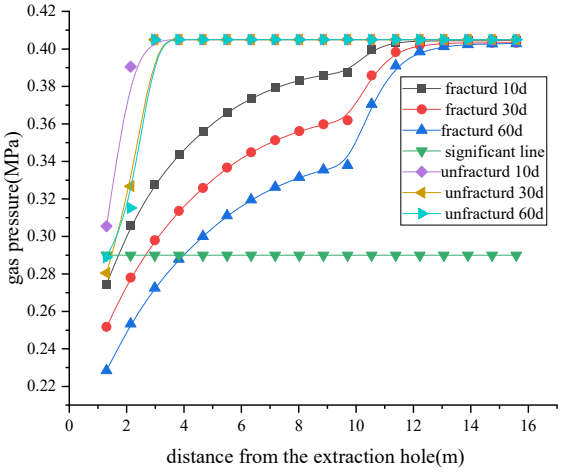

Fig. 4. Variation of gas pressure with extraction distance

Under conditions with unfractured coal, the effective extraction radii at 10, 30, and 60 days are 0.8 m, 1.4 m, and 1.6 m, respectively. In contrast, after hydraulic fracturing, the effective extraction radii at these intervals increase to 1.8 m, 2.4 m, and 3.9 m, respectively. After 60 days of pumping, the effective extraction radius is 2.44 times greater than the radius observed without fracturing.

4. Industrial test

4.1. Test drilling construction design

Based on the simulation outcomes and the geological conditions at the 24130 working face of Pingdingshan No. 10 coal mine, parallel boreholes were drilled along the coal seam at a specified distance from the inlet roadway. For the test, a total of 7 drill holes, each with a diameter of 94 mm, were established, as depicted in Fig. 5. The hydraulic fracturing device used in the test is illustrated in Fig. 6. The initial pressure of the device was set to 5 MPa, which was then gradually increased to 10 MPa after passing inspection, and maintained for a period. The operation was monitored through nearby control drilling holes, and the hydraulic fracturing process was concluded when the water flow in the borehole became clear.

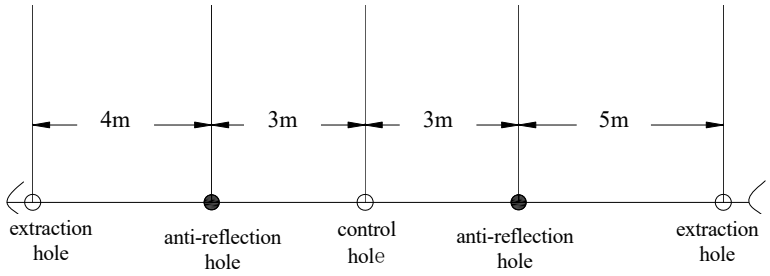

Fig. 5. Borehole layout

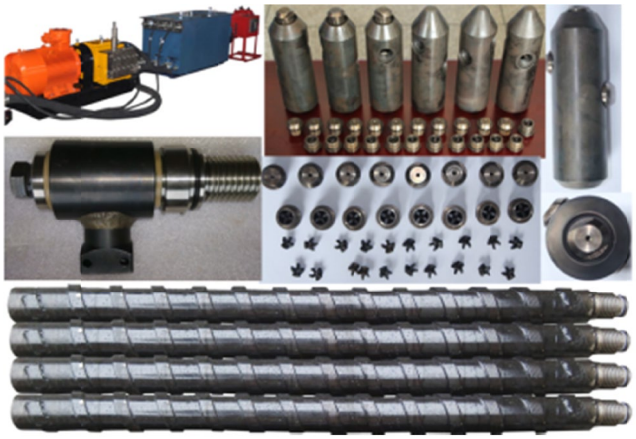

Fig. 6. Hydraulic fracturing plant

4.2. Description of field test effect

The goal of hydraulic fracturing is to enhance the formation of cracks within the coal body, thereby creating pathways for gas flow and improving coal seam permeability. To evaluate the effectiveness of the fracturing process, gas flow and concentration are key indicators. After completing each extraction borehole, a monitoring device is installed to record gas flow and concentration parameters for both conventional and test drilling.

Using ORIGIN software to analyze the data, Fig. 7 presents the gas concentration and purity variations in the extraction holes. Post-fracturing, the gas concentration in the test boreholes ranges from 36.9% to 55.4%, with gas purity between 0.0059 m^3/min and 0.0132 m^3/min. The average gas concentration is 42.4% and the average gas purity is 0.0098 m^3/min. In contrast, conventional boreholes show gas concentrations ranging from 5.4% to 38.5%, and gas purity from 0.0014 m^3/min to 0.0039 m^3/min, with average values of 15.4% and 0.0018 m^3/min, respectively. Thus, hydraulic fracturing results in a 2.75-fold increase in average gas concentration and a 5.44-fold increase in average gas purity compared to conventional methods, highlighting the significant effectiveness of the directional hydraulic fracturing technique.

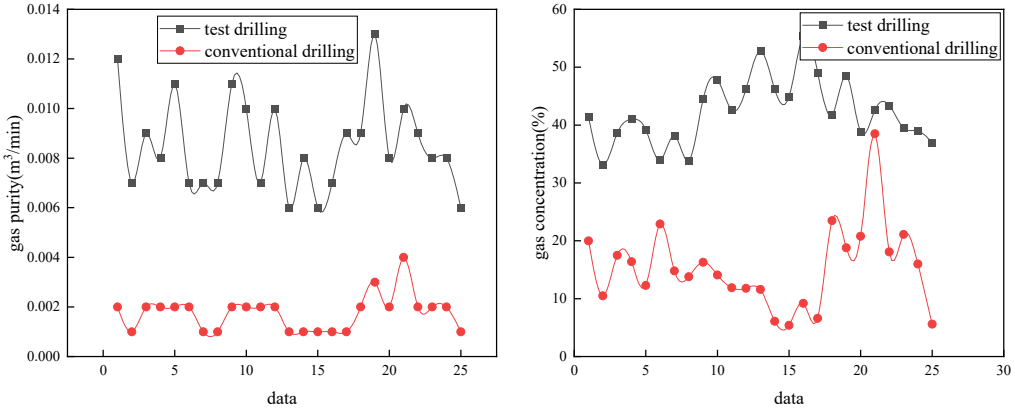

(a) gas purity (b) gas concentration

Fig. 7. Curve of gas parameters in extraction hole

4.3. Effective extraction radius

The effective extraction radius of hydraulic fracturing is calculated according to the formula below [18]:

$$R_c \le \sqrt{\frac{Q_c}{L\rho W \pi\eta}} (\eta \ge 30\%) \tag{8}$$

Where, W is the original gas content of coal seam, m^3/t; Q_c is the cumulative extraction pure quantity; ρ is the density of coal, t/m^3; R_c is the effective extraction radius, m; L is the effective borehole length, m. π is the porosity of coal.

The actual gas content measured at the 24130 working face of Pingdingshan 10# mine is 8.48m^3/t, and the length of effective extraction borehole is 50 m. The effective extraction radius calculated according to formula (8) is shown in TABLE 2. It can be seen from the data fitting in TABLE 2 that the fitting formula for the effective pumping radius of hydraulic fracturing is $R_c = 0.489t^{0.4871}$. When the pumping time is 60 days, the effective pumping radius is 3.6 m, which is roughly consistent with the numerical simulation results and verifies the effectiveness of the numerical simulation model. According to the extraction data of the 24130 working face of Pingdingshan 10# mine before fracturing, it can be calculated that when the extraction radius reaches 3.0 m, it takes 84 days to pump, while after hydraulic fracturing, the extraction radius can reach 3.0 m in only 41 days, and the extraction time is shortened by 43 days.

TABLE 2

Effective extraction radii of hydraulic fracturing drilling with different pre-pumping times

Time/d	10	20	30	40	50	60
Effective extraction radius/m	1.5	2.1	2.6	2.9	3.3	3.6

5. Conclusion

(1) A coupled model integrating hydraulic fracturing with coal rock stress-damage-permeability was developed using COMSOL Multiphysics. This model analyzed the distribution of the coal seam's elastic modulus, changes in permeability, and stress alterations before and after fracturing. Results showed that after 1800 seconds of hydraulic fracturing, the extraction pressure rapidly dropped to the effective pressure extraction line, and the effective extraction radius increased by 2.44 times compared to pre-fracturing conditions after 60 days.

(2) In the pilot test conducted at the 24130 working face of Pingdingshan 10# mine, the directional hydraulic fracturing increased the gas concentration by 2.75 times and the pure gas extraction volume by 5.44 times compared to conventional drilling methods.

(3) Directional hydraulic fracturing at working face 24130 in Pingdingshan 10# mine meets the effective extraction radius formula of $R_c = 0.489t^{0.4871}$. When the extraction radius is 3.0 m, the extraction time after the fracturing operation is 41 days, which is 43 days shorter compared with the extraction time of conventional extraction holes.

Declaration of Competing Interest

The authors declare that they have no known competing financial interests or personal relationships that could have appeared to influence the work reported in this paper.

Acknowledgement

This paper is financially supported by the Natural Science Foundation of China (No. 52374202). The authors declare that there is no conflict of interest regarding the publication of this paper.

References

[1] Z.P. Wang, Z. L. Ge, R.H. Li, et al., Coupling effect of temperature, gas, and viscoelastic surfactant fracturing fluid on the microstructure and its fractal characteristics of deep coal. Energ. Fuel **35** (23), 19423-19436 (2021).

[2] Q. Huang, S. Liu, W. Cheng, et al., Fracture permeability damage and recovery behaviors with fracturing fluid treatment of coal: an experimental study. Fuel **2**, 118809 (2020).

[3] F. Awan, A. Keshavarz, H. Akhondzadeh, et al., Stable dispersion of coal fines during hydraulic fracturing flowback in coal seam gas reservoirs – an experimental study. Energ. Fuel **34**, 5566-5577 (2020).

[4] J. Nian, B. Zhao, W. Zhang, Numerical simulation research on the pressure relief and permeability enhancement mechanism of large-diameter borehole in coal seam. Geofluids, 2022 (2022).

[5] C. Zhang, Q. Bai, Y. Chen, Using stress path-dependent permeability law to evaluate permeability enhancement and coalbed methane flow in protected coal seam: a case study. Geomechanics and Geophysics for Geo-Energy and Geo-Resources **6**, 1-25 (2021).

[6] L. Zhang, S. Chen, C. Zhang, et al., The characterization of bituminous coal microstructure and permeability by liquid nitrogen fracturing based on μCT technology. Fuel **262**, 116635 (2020).

[7] X. He, K. Yang, P. Han, et al., Permeability enhancement and gas drainage effect in deep high gassy coal seams via long-distance pressure relief mining: a case study. Appl. Mech. Mater. 2021, 1-13 (2021).

[8] R.L. Johnson, B. Glassborow, M.P. Scott, et al., Utilizing current technologies to understand permeability, stress azimuths and magnitudes and their impact on hydraulic fracturing success in a coal seam gas reservoir [C]//SPE Asia Pacific Oil and Gas Conference and Exhibition. OnePetro (2010).

[9] Q. Hu, L. Liu, Q. Li, et al., Experimental investigation on crack competitive extension during hydraulic fracturing in coal measures strata. Fuel **265**, 117003 (2020).

[10] Y. Lu, F.Yang, Z. Ge, et al., Influence of viscoelastic surfactant fracturing fluid on permeability of coal seams. Fuel **194**, 1-6 (2017).

[11] D. Li, Y. Chen, J. Zhang, et al., Research and application of pressure relief and permeability improvement in high gas outburst mines by directional drilling and hydraulic jet. Front. Earth. Sci. **10**, 1029429 (2023).

[12] L. Wang, Z. Lu, D. Chen, et al., Safe strategy for coal and gas outburst prevention in deep-and-thick coal seams using a soft rock protective layer mining. Safety. Sci. **129**, 104800 (2020).

[13] Y. Cao, J. Zhang, H. Zhai, et al., CO_2 gas fracturing: A novel reservoir stimulation technology in low permeability gassy coal seams. Fuel **203**, 197-207 (2017).

[14] X.H. Zhou, L.J. Zhou, C.J. Fan, et al., Simulating and experimental study on enhancing gas drainage from low permeability coal seam by hydraulic fracturing. China Safety Science Journal **27**, 81-86 (2017).

[15] H.F. Ma, Z.H. Cheng, K.X. Zhang, et al., Intensive permeability enhancement experiment through hydraulic fracturing by way of wa-ter-sand-water in kilometer deep well with high gas seam. Journal of China Coal Society **42**, 1757-1764(2017).

[16] M. Profit, M. Dutko, A. Bere, et al., Effect of Interbeds on Hydraulic Fracture Characteristics and Formation Pressure Response [C]//Unconventional Resources Technology Conference, Houston, Texas, 23-25 July 2018. Society of Exploration Geophysicists, American Association of Petroleum Geologists, Society of Petroleum Engineers. 1258-1277 (2018).

[17] H. Marsden, S. Basu, A. Striolo, et al., Advances of nanotechnologies for hydraulic fracturing of coal seam gas reservoirs: Potential applications and some limitations in Australia. International Journal of Coal Science & Technology **9**, 27 (2022).

[18] J.Z. Jia, J.Q. Ge, W.H. Zhen, et al., Research and application of anti-reflection technology of hydraulic fracturing. China Safety Science Journal **30**, 63-68 (2020).

[19] S. Li, C. Fan, J. Han, et al., A fully coupled thermal -hydraulic mechanical model with two-phase flow for coalbed methane extraction. J. Nat. Gas. Sci. Eng. **33**, 324-336 (2016).

[20] F. Reng, Research on anti-reflection measures of hydraulic reaming of low permeability soft coal seam in Goutou coal mine[C]//IOP Conference Series: Earth and Environmental Science. IOP Publishing **768**, 012026 (2021).